RESEARCH PAPER

Chemical Co-precipitation Synthesis of Manganese Ferrite (MnFe$_2$O$_4$) and Evaluation of Its Applications in Copper Removal from Aqueous Solutions

Shima Shahidizandi [1], Hossein Mohammadi-Manesh [1], Mohammad Mohsen Loghavi [2]*

[1] *Department of Chemistry, Faculty of Science, Yazd University, Yazd, Iran*

[2] *Department of Energy Storage, Institute of Mechanics, Shiraz, Iran*

ARTICLE INFO

ABSTRACT

This study investigated the removal of copper from aqueous solutions using manganese ferrite (MnFe$_2$O$_4$) nanoparticles as a suitable and new adsorbent. For this purpose, manganese ferrite nanoparticles were synthesized by the co-precipitation method, and the effect of pH parameter, contact time, adsorbent concentration, as well as the influence of initial concentration on the copper adsorption process in the batch system were studied. To determine the properties of manganese ferrite nanoparticles, a scanning electron microscope, X-ray diffraction device, and infrared spectrometer were used. The results showed that the average size of these nanoparticles was between 30 and 50 nm. Moreover, it was indicated that by increasing the pH of the aqueous solution from 3 to 7, the adsorption capacity of copper increased so that at an optimal pH of 7, the adsorption rate reached more than 99%. Furthermore, increasing the contact time and the amount of adsorbent increased the removal efficiency, and the results revealed that with increasing the concentration of copper, the adsorption capacity increased. In the study of adsorption isotherms, the experimental data showed more agreement with the Freundlich model with an adsorption capacity of more than 199 mg/g. In addition, the data obtained for the adsorbent indicated that the copper adsorption follows the pseudo-second-order kinetic model. In general, the results of this study showed that the use of manganese dioxide nanoparticles is a suitable method with a high potential for removing copper from aqueous solutions.

How to cite this article

INTRODUCTION

The existence of safe and reliable water sources without toxic and dangerous pollutants is the basic and essential need for a healthy and sustainable life. Heavy metals are among the water pollutants discharged from municipal wastewater, sludge from wastewater treatment, and imported into the environment. They accumulate in ecological systems, and their gradual increase in concentration causes several adverse effects on the systems. The degree of toxicity of metals in different conditions, and is the function of factors

* *Corresponding Author Email: mohammadimanesh@yazd.ac.ir*

such as concentration, environmental conditions, contact time, and other physical, chemical, and biological factors [1]. Copper is one of the essential elements for plants and animals; however, in large quantities, it is toxic to all living organisms [2]. If a significant amount of copper is entered into the body, it interferes with the absorption of Iron and Zinc. It also causes anemia and iron deficiency and harms fertility [3,4]. The WHO (World Health Organization) has set a limit of 1.5 mg per liter of copper in municipal water.

There are several methods for removing heavy metals from water and wastewater. The most important methods used for this purpose are chemical deposition, ion-exchange (IE), reverse osmosis (RO), membrane filtration (MF), solvent extraction (SE), and adsorption. The disadvantage of these methods is the need for the costly and time-consuming pretreatment processes for the removal of suspended solids. One of the main solutions to eliminate the shortcomings of conventional treatment methods is the use of nanotechnology, which is the process that plays a key role in preventing contamination, identification, measurement, and treatment of pollutants.

Due to their small size, large cross-section, crystalline shape, unique lattice order, and therefore high reactivity, nanoparticles can be used to purify and convert pollutants into less harmful materials [5]. The adsorption process by metal nanoparticles is one of the environmentally friendly technologies that researchers have considered in recent years as an effective factor in removing heavy metals from water and wastewater [6].

Recent studies show that manganese ferrite nanoparticles have played an effective role in removing heavy metals from aqueous solutions due to their high adsorption capacity and selectivity [7,8]. Yuming Ren et al. used manganese dioxide nanoparticles to adsorb copper and lead. Their results revealed that the experimental data followed the pseudo-second-order adsorption kinetics, and in the studies on adsorption isotherm, the results followed the Langmuir adsorption isotherm [9]. Moreover, Chaolo et al. used manganese ferrite nanoparticles functionalized with multi-walled carbon nanotubes to remove cadmium, and their results indicated that the contact time was 150 minutes as the equilibrium time [10]. In addition, Shi and Dong evaluated the adsorption of chromium and copper elements with magnetic nanoparticles. According to their results, the copper adsorption increased by increasing the pH from 1 to 5 [11]. The present study aimed to synthesize manganese ferrite nanoparticles by chemical co-precipitation synthesis and determine the effect of contact time, nanoparticle concentration, and initial copper concentration on copper's efficiency and adsorption capacity by manganese ferrite nanoparticles from aqueous solutions.

MATERIALS AND METHODS

Synthesis of manganese ferrite and its characterization

Manganese (II) chloride tetrahydrate (MnCl$_2$·4H$_2$O, Merck), Iron (II) chloride tetrahydrate (FeCl$_2$·4H$_2$O, Merck), Iron (III) chloride hexahydrate (FeCl$_3$·6H$_2$O, Merck), and Ammonia solution 25% (NH$_4$OH, Merck) were used for the synthesis of manganese ferrite nanoparticles. All reagents were used as received without further purification.

In the co-precipitation method, reagents were prepared according to the literature. This process involves the precipitation of Fe^{2+} and Fe^{3+} salt (e.g., chlorides, sulfates, and nitrates) in aqueous solutions by adding a base (e.g., NaOH) [12]. For this purpose, an aqueous solution of precursors (MnCl$_2$, FeCl$_2$, and FeCl$_3$) with a preset stoichiometry was prepared by an overhead stirrer (IKA Nanostar 7.5 digital). The temperature of the solution was then increased to 80. While the solution was stirred at 450 rpm, ammonia was gradually added to the solution for 20 minutes to adjust the pH and precipitate the dark brown manganese ferrite particles. Finally, the obtained oxide samples were used for characterization. Scanning Electron Microscope (SEM), X-ray diffraction device and infrared spectrometer were used to characterize the produced manganese ferrite nanoparticles.

Investigation of cu^{2+} adsorption by manganese ferrite

In this study, manganese ferrite nanoparticles were first synthesized and used, and all adsorption experiments were performed in a batch system. To prepare a standard solution of copper, 3.8 g of copper nitrate (Cu(NO$_3$)$_2$ .3H$_2$O) was poured into 1000ml of distilled water, and a solution of 1000 mg/l of copper was prepared. Afterward, copper solutions were prepared with different

concentrations by diluting the standard solution. The pH of the solution was adjusted with hydrochloric acid and a gain of 0.1 M. Moreover, the removal of copper from aqueous solutions was investigated by manganese ferrite nanoparticles at different pH, contact times, nanoparticle concentrations, and contaminant concentrations.

To determine the optimal pH of copper removal, the pH of the solution was adjusted in the range of 3 to 7 using the two mentioned substances. The effect of contact time on copper removal by manganese ferrite nanoparticles was performed at times of 5 to 120 minutes at the optimum pH obtained in the previous experiment [13].

To investigate the effect of nanoparticle concentration on removal efficiency and determine the optimal concentration of nanoparticles for copper removal from aqueous solutions, the concentrations of 0.15 to 0.5 g/l were taken into account [14].

Moreover, to determine the effect of different concentrations of copper on the adsorption process, discontinuous experiments were considered in 100 ml containers with concentrations of 10-75 mg/l copper [13].

During the reaction time, the container was placed on a vibrating device at a speed of 160 rpm. After the test, the contaminated manganese ferrite nanoparticles were separated from the solution using a centrifuge of Model 5810R (Eppendorf, Germany). Finally, the obtained solution was isolated, and the amount of copper inside the solution was read by an atomic absorption device of the solar model (Flame-AAS, Perkin Elmer PE4000). The efficiency (percentage) of heavy metal (Copper) removal was calculated from Equation 1, and its equilibrium adsorption capacity by manganese ferrite nanoparticles was obtained from Equation 2.

$$R = \frac{C_0 - C_e}{C_0} \times 100 \tag{1}$$

$$q = \frac{C_0 - C_e}{C_0} \times 100 \tag{2}$$

Where R is the percentage of removal or removal efficiency of copper, q implies the adsorption capacity or the amount of adsorbed ions in milligrams per gram. C_0 and C_e denote the initial and final concentrations of copper in milligrams per liter, respectively, m is the adsorbent mass in grams, and V denotes the volume of solution in liters.

Adsorption kinetics relationships

One of the most important factors for the design of the adsorption system is to predict the speed of the adsorption process, which is controlled by the system's kinetics. The kinetic studies of copper adsorption from aqueous solutions by manganese ferrite nanoparticles were investigated using pseudo-first-order and pseudo-second-order kinetic models.

Pseudo-First-Order Kinetics Equation

According to Equation 3, in the pseudo-first-order kinetic equation, the adsorption rate is proportional to the empty sites [15].

$$\frac{dq_t}{d_t} = -k_1(q_e - q_t) \tag{3}$$

By applying logarithm to Equation 3, a pseudo-first equation, also known as the Lagergren relation, is formed as follows:

$$(q_e - q_t) = Log q_e - \frac{k_1 t}{2.303} \tag{4}$$

Where q_e is the adsorption capacity in equilibrium (mg/g), q_t is the adsorption capacity in time (mg/g), K_1 is the pseudo-first-order velocity constant in 1 minute and t is the time in minutes.

Pseudo-Second-Order Kinetic Equation

According to Equation 5, in the pseudo-second-order kinetic equation, the adsorption rate is proportional to the square of the empty sites [16].

$$\frac{dq_t}{q_t} = \frac{1}{k_2 q_e^2} - (q_e - q_t)^2 \tag{5}$$

By applying logarithm to Equation 5, a pseudo-second relation or Ho relation is formed as follows:

$$\frac{t}{q_t} = \frac{1}{k_2 q_e^2} + \frac{t}{q_e} \tag{6}$$

Where k_2 is a pseudo-second velocity constant in grams in mg/min. The kinetic relationships of copper adsorption from aqueous solutions are shown in Table 1.

Isotherms of surface adsorption

The adsorption temperature curve is the

equilibrium relationship between the adsorbed concentration in the fluid phase (C) and the adsorbed concentration on solid particles (q) at a given temperature.

Langmuir Equilibrium Isotherm

The simplest theory for monolayer adsorption is the Langmuir model, proposed in 1916. In the Langmuir model, it is assumed that adsorption on places is homogeneous and adsorption is monolayer [17]. In this model, molecules are adsorbed on well-defined surface locations, and each site can only adsorb one adsorbed molecule [18]. The Langmuir equation is expressed in Equation 7 as follows [12].

$$q_e = \frac{bp_mC_e}{1 + bC_e} \tag{7}$$

The linear form of Equation 7 is as follows:

$$\frac{C_e}{q_e} = \frac{1}{q_mb} + \frac{C_e}{q_m} \tag{8}$$

Where, C_e denotes the equilibrium concentration of the solution (mg/l), q_e is the absorption capacity in equilibrium terms (mg/g), q_m (mg/g) and b (l/mg) are factors related to adsorption capacity and absorption energy, respectively, obtained by plotting C_e/q_e versus C_e.

Freundlich Equilibrium Isotherm

The Freundlich model assumes that adsorption is reversible on heterogeneous sites, and this model is suitable for multilayer adsorption [17,18]. The Freundlich isotherm is defined as Equation 9 [19].

$$q_e = k_f \, C_e^{\frac{1}{n}} \tag{9}$$

By applying logarithm to both sides of the equation in linear form, Equation 10 is formed as follows:

$$Logq_e = Logk_f + \frac{1}{n}LogC_e \tag{10}$$

Where K_f and n are the coefficients related to adsorption capacity and adsorption intensity, respectively, which are obtained by plotting the Log q_e versus Log C_e. The isothermal relationships of copper adsorption from aqueous solutions are indicated in Table 1.

RESULTS AND DISCUSSION

Properties of manganese ferrite nanoparticles

Fig. 1 indicates an image of the nanoparticles used by the SEM device. This figure shows that manganese ferrite nanoparticles are in the form of nanoparticles that are aggregated and completely adhered to each other. The size of the observed nanoparticles is in the range of 30-50 nm. Fig. 2 indicates the XRD pattern, and the peaks observed in these spectra correspond to the α and γ phases of manganese ferrite.

The XRD pattern does not show any peaks related to the inserted hydroxide or nitrate, indicating the complete removal of structural water and nitrate ions during heat treatment. In general, it can be expressed that manganese dioxide prepared in this method has two dominant phases α and γ [20,21]. The synthetic samples in the range of 400 to 4000 cm⁻¹ of FT-IR spectrum were taken to identify synthetic products better and confirm XRD results.

Fig. 4 indicates the spectrum of manganese ferrite nanoparticles. The important points in this spectrum show that the peaks observed in 3450-3460 cm⁻¹ and 1630-1640 cm⁻¹ confirm the presence of surface water in these samples. The

Table 1. Synthetic equations of isotherm of copper adsorption from aqueous solutions

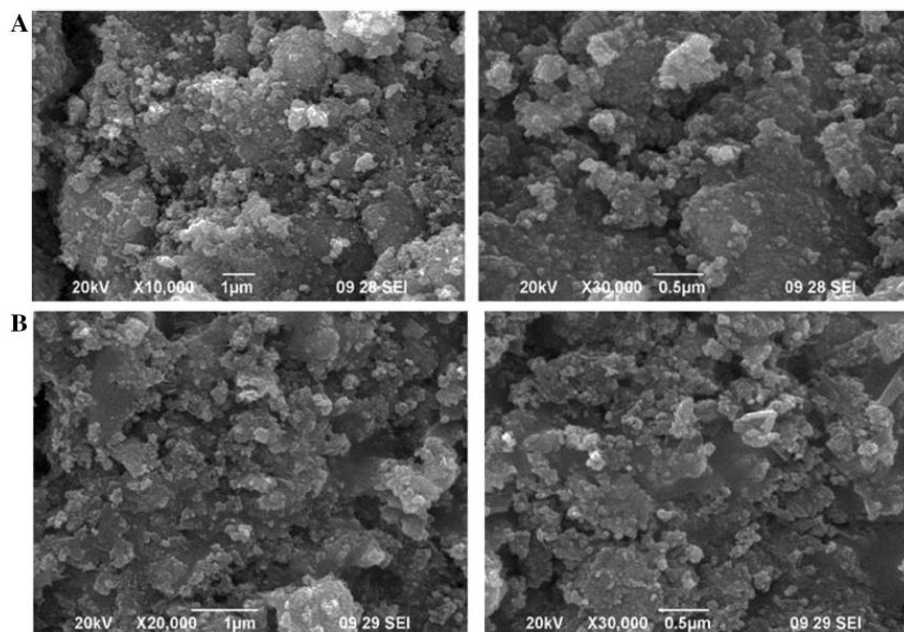|	Equation	Linear Form
Pseudo-first-order Kinetics	$\frac{dq_t}{dt} = -k_1(q_e - q_t)$	$(q_e - q_t) = logq_e - \frac{k_1t}{2.0303}$
Pseudo-second-order Kinetics	$\frac{dq_t}{dt} = -k_2(q_e - q_t)^2$	$\frac{t}{q_t} = \frac{1}{q_2q_e^2} + \frac{t}{q_e}$
Langmuir Isotherm	$q_e = \frac{bq_mc_e}{1 + bC_e}$	$\frac{c_e}{q_e} = \frac{1}{q_mb} + \frac{c_e}{q_m}$
Freundlich Isotherm	$q_e = k_fc_e^{\frac{1}{n}}$	$logq_e = logk_f + \frac{1}{n}logc_e$

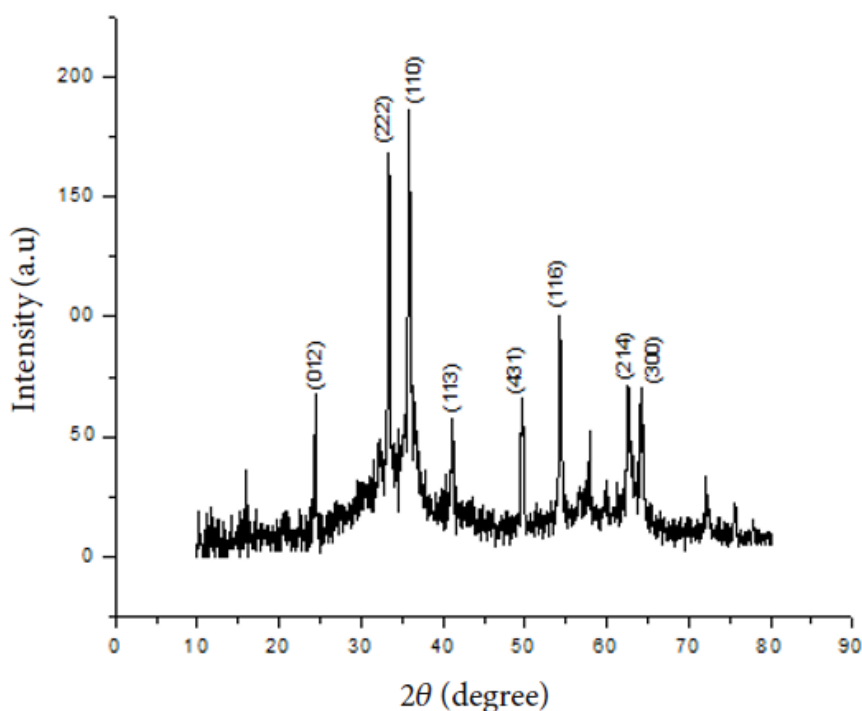Fig. 1. a SEM image of pure Fe_3O_4. b SEM image of Mn^{2+} doped Fe_3O_4

Fig. 2. XRD image of iron oxide (Fe_3O_4)

absence of peaks related to the vibrations of the nitrate group in the range of 1390-1385cm^{-1} indicates the complete removal of nitrate due to heat treatment. The peaks observed in 1520-1530 cm^{-1} and 1395-1410 cm^{-1} belong to the carbonate group, which are probably absorbed through the air by the samples (reaction of hydroxide with CO_2 of air). The peaks observed at 560-580 cm^{-1}
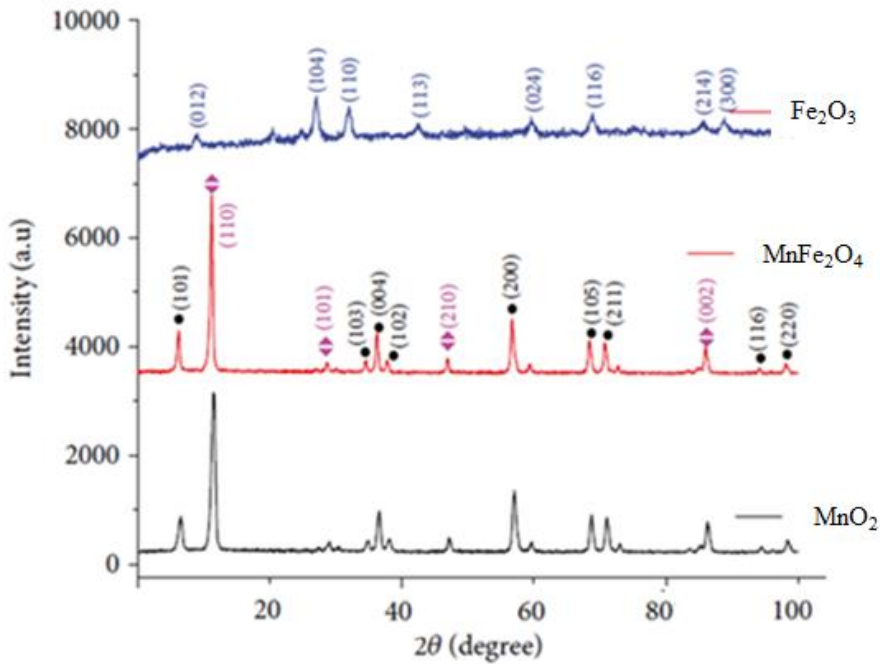
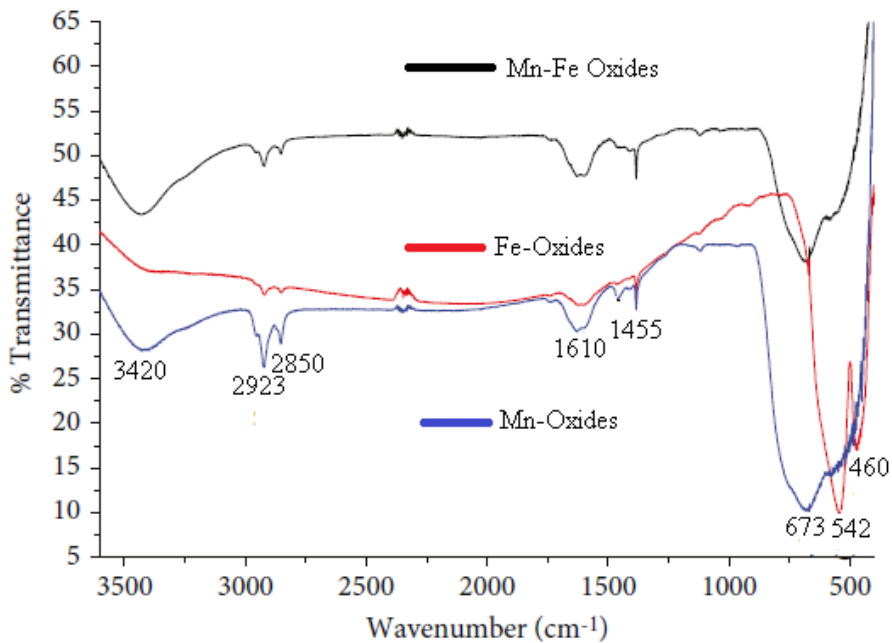Fig. 3. XRD spectra of corresponding metal oxide nanoparticles

Fig. 4. FT-IR spectrum of corresponding metal oxide nanoparticles

are related to the Mn-O-Mn vibrational model and confirm the oxidation of these samples [22].

Effect of different factors on copper removal

efficiency by manganese ferrite nanoparticles
Effect of pH on copper removal efficiency

The effect of pH of aqueous solution on the removal efficiency of copper by manganese ferrite

nanoparticles was performed by changing the pH of the aqueous solution from 3 to 7 for 120 minutes, the initial concentration of the contaminant is 10 mg/l, and the amount of adsorbent is 0.25 g/l. Fig. 5 shows the effect of different pHs on copper removal. This figure shows that manganese ferrite nanoparticles are less efficient at refining copper at low pHs. The adsorption efficiency and capacity of copper at pH=3 are at their lowest values (52.1% and 20.84 mg/g, respectively).

By increasing the pH from 3 to 7, the percentage of removal and copper adsorption capacity increased and reached its maximum of 96.6% and 38.64 mg/g, respectively; therefore, the pH=7 was selected as the optimal pH for copper removal. At low pHs, the concentration of H+ ions in solution is high, causing competition between Cu^{2+} ions and H^+ ions for adsorption in adsorbent voids. In deionized water, copper species are present in the forms of $Cu(OH)^{2+}$, $Cu(OH)^+$, Cu^{2+}, and $Cu(OH)_2$ [23].

The concentration of hydrolyzed species depends on the concentration of copper and the pH of the solution, and Cu^{2+} ions are the only ion species present in the solution at a pH of less than 6 [24]. At acidic pHs of 2 and 3, the carbonyl groups on the surface of the adsorbent particles create a positive charge and repel Cu^{2+} ions. There is also competition between the H ions in the medium and the Cu^{2+} ions for adsorption on the side, which reduces the amount of adsorption. At pHs of 5, 6, and 7, due to the increased amount of OH in the environment, the percentage and adsorption

capacity of Cu^{2+} cations increases [25,26]. Hero et al. used manganese ferrite hydrogen peroxide nanoparticles at an optimal pH=7 to achieve the removal of approximately 99% of the iron metal [27]. Moreover, Shi and Dong evaluated the adsorption of chromium and copper elements with magnetic nanoparticles. The results of other studies have also indicated that copper adsorption increases by increasing the pH from 1 to 5 [11].

Effect of contact time on copper removal efficiency

The effect of reaction time was investigated on copper removal efficiency using manganese ferrite nanoparticles by changing the contact time from 0 to 120 minutes in a solution with pH=7, initial concentration of pollutant equal to 10 mg/l, and adsorbent amount of 0.25 g/l. Fig. 6 indicates a graph of copper removal at regular intervals by manganese ferrite nanoparticles. The results showed that the percentage of copper adsorption increased with increasing the contact time. This process lasted 60-90 minutes until it reached equilibrium time. At this time, the copper removal efficiency reached 96.8%.

After this period, the adsorption rate decreased and led to a smooth and continuous curve. This figure shows that in short times, large amounts of metal are adsorbed by the adsorbent so that a significant part of the adsorption (approximately 90% adsorption) was in the first 30 minutes of the adsorption phase. In general, as the reaction time increases, the contact time between the pollutant ions and the nanoparticles increases, and the
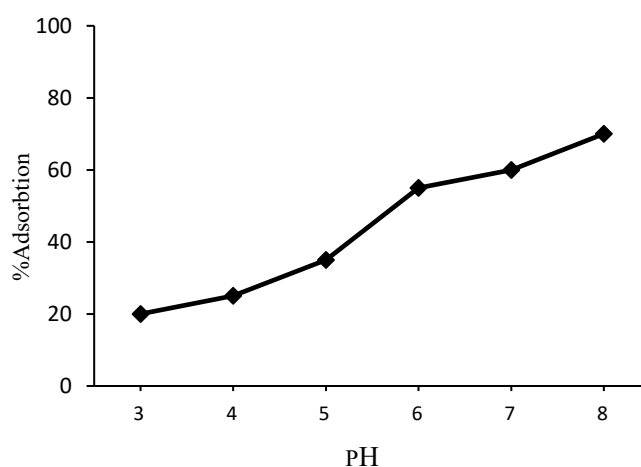

Fig. 5. Effect of pH on adsorption capacity of copper removal by manganese ferrite nanoparticles (initial concentration: 10 mg/l, adsorbent amount: 0·25 g/l, contact time: 120 minutes)
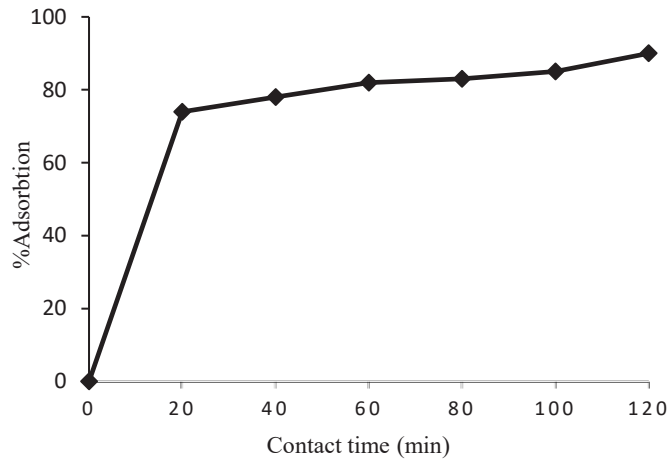
Fig. 6. Effect of different times on the removal efficiency and adsorption capacity of copper by manganese ferrite nanoparticles (initial concentration: 10mg/l, adsorbent concentration: 0.25 g/l, pH=7)

ions have more time to bind to the adsorption sites on the particle surfaces. Yuming Ren et al. used manganese dioxide nanoparticles to adsorb copper and lead. In this study, 120 minutes was appropriate as the required time to achieve balance [9].

Moreover, Donglin Zhao et al. used manganese ferrite nanoparticles to remove lead. The results indicated that with increasing the contact time, the amount of lead absorption increased, and the time of 1 h was obtained as the equilibrium time [28].

Effect of adsorbent amount on copper removal efficiency

The effect of the adsorbent amount was investigated on copper removal efficiency using manganese ferrite nanoparticles by changing the amount of nanoparticles from 0.15 to 0.5 g/l in a solution with pH=7 and the optimal contact time obtained from the previous experiment (60 minutes) and initial concentration of contaminant equal to 10 mg/l. Fig. 7 indicates the effect of the amount of adsorbent on the removal percentage and adsorption capacity of copper ions by
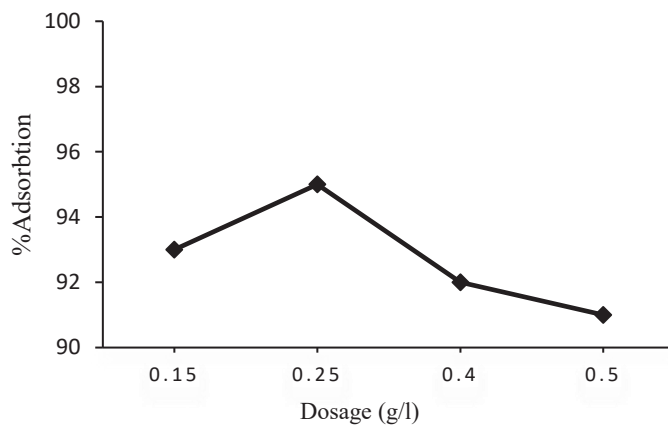

Fig. 7. Effect of initial concentration adsorption capacity of copper by manganese ferrite nanoparticles (adsorbent amount: 0.5g/l, contact time: 90min, pH=7)
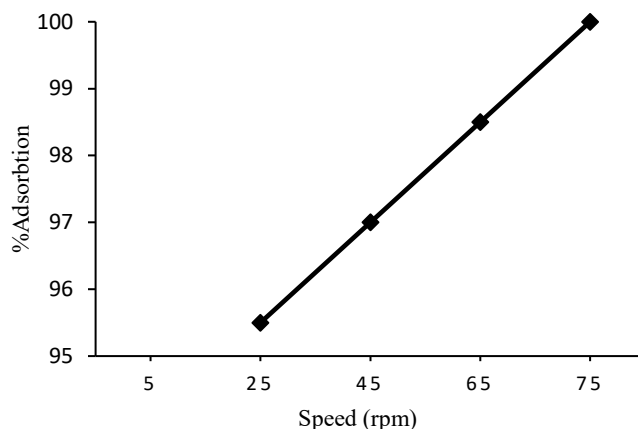
Fig. 8. Effect of initial concentration adsorption capacity of copper by manganese ferrite nanoparticles (adsorbent amount: 0.5g/l, contact time: 90min, pH=7)

manganese ferrite nanoparticles. By increasing the adsorbent from 0.15 g/l to 0.5 g/l, the removal efficiency increased from 92.7% to 97.2% and the adsorption capacity decreased from 61.8 mg/g to 19.44 mg/g. In addition, by increasing the amount of adsorbent from 0.25 g/l to 0.5 g/l, no significant change was observed in the efficiency and adsorption capacity of copper.

As the amount of adsorbent increases, the removal efficiency increases; however, the adsorption capacity decreases because the initial concentration is constant, and with further increase in adsorbent, the full adsorption capacity of the adsorbent is not used, and there are free adsorption sites on the print concentration (g/l). The amount of adsorbent depends on the removal efficiency and adsorption capacity of copper by manganese dioxide nanoparticles (initial concentration of 10 mg/l, contact time of 90 minutes, and pH=7 on the adsorbent surface). In other words, increasing the copper removal

efficiency by increasing the adsorbent dose is due to the increase and availability of exchange sites and special surfaces [29,30]. Meng Soo et al. conducted a study to adsorb lead using hydrogen manganese ferrite particles and concluded that as the adsorbent increases, the removal percentage increases as well [31].

In addition, Shihabudheen et al. used manganese ferrite nanoparticles and reported that with increasing adsorbent, the removal efficiency increases but the adsorption capacity decreases [32].

Effect of initial concentration on copper removal efficiency

The effect of the initial concentration of pollutants was investigated on the removal efficiency of copper using manganese ferrite nanoparticles and by changing the concentration of 10, 25, 50, and 75 mg/l pollutants in a solution with pH=7, the amount of 0.5 g/l nanoparticles

Table 2. Parameters obtained in pseudo-first and second-order copper models

The pseudo-first-order model equation	R^2	K$_1$	q$_e$(mg/g)
Y=-0.0131x+0.7274	0.9592	0.0301	5.338
The pseudo-second-order model equation	R^2	K$_2$	q$_e$(mg/g)
Y=0.0255x+0.0375	39.215	0.0173	0.9998

and in 60 minutes. Fig. 8 indicates the effect of different concentrations of copper on the removal efficiency by manganese dioxide nanoparticles. With increasing initial copper concentration, the adsorption capacity of copper by manganese ferrite nanoparticles increased from 19.48 to 147.6 mg/g, and it was shown that when the initial copper concentration increases, there was a lack of surface and active sites for adsorption. At high concentrations, it causes less adsorption, this level and sites are constant, and when the concentration increases, the surface and sites fill, and the adsorption capacity increases [33].

In this study, with increasing the initial concentration of copper, the removal efficiency increased as well, the reason which was that the initial concentrations applied in this study was far from the final adsorption capacity; therefore, as the initial concentration increases, the adsorption increases in the same proportion, and as the concentration increases from one concentration to the next percentage, the removal is reduced. Yuming Ren et al. used manganese ferrite nanoparticles for copper removal and obtained similar results [9].
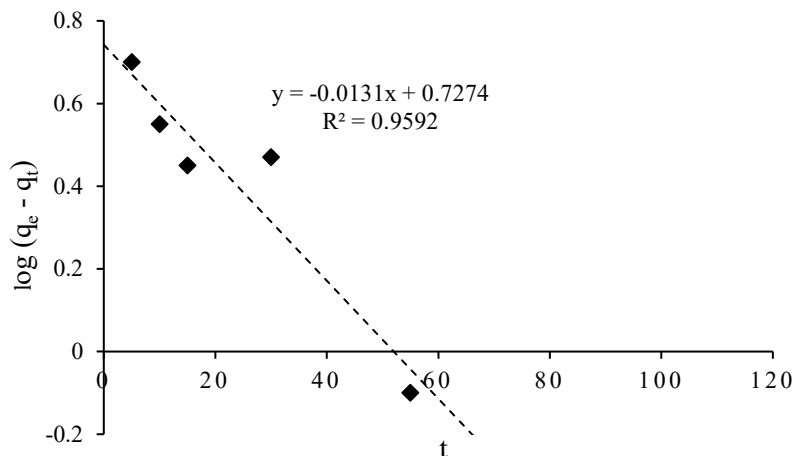
Moreover, Meng Soo et al. worked on the

$$y = -0.0131x + 0.7274$$
$$R^2 = 0.9592$$

Fig. 9. Pseudo-first-order kinetics diagram of copper adsorption by manganese ferrite nanoparticles
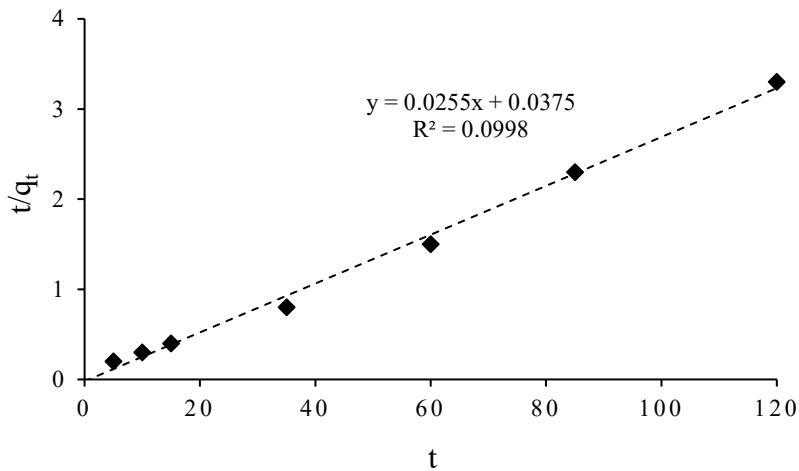

$$y = 0.0255x + 0.0375$$
$$R^2 = 0.0998$$

Fig. 10. Pseudo-second-order kinetics diagram of copper adsorption by manganese ferrite nanoparticles

adsorption of lead using manganese ferrite particles and concluded that as the initial concentration of lead increases, the adsorption capacity increases as well [31].

Copper adsorption kinetics

Adsorption kinetics are used to determine the control mechanism of adsorption processes. To understand the dynamics of the reaction and predict the adsorption state with time, it is essential to know the kinetics of the processes [34,35].

The results of kinetic experiments of copper adsorption from aqueous solutions by manganese ferrite nanoparticles using pseudo-first-order and pseudo-second-order kinetic models are shown in Table 2. As indicated in these tables, the coefficient of determination (R) in the pseudo-second-order model is higher than the first-order pseudo-model, which indicates that the second-order pseudo-model has more capability than the first-order pseudo-model in fitting the removal data related to copper from aqueous solutions (Fig. 9 and Fig. 10). The results of Moradi's investigation conducted on the removal of copper and lead from aqueous solutions using magnetic iron oxide nanoparticles show that both metals follow the relationship of H$_0$ adsorption kinetics [36]. In addition, Donglin et al. used manganese dioxide nanoparticles and indicated that kinetic studies of
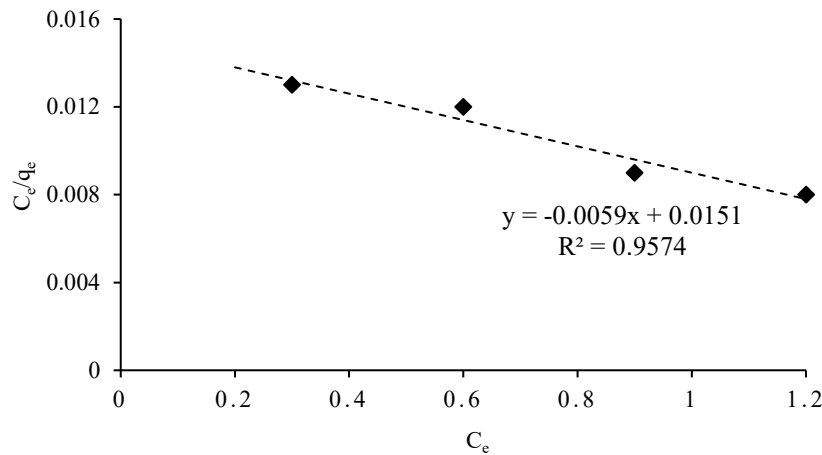

Fig. 11. Langmuir isotherm diagram of copper adsorption by manganese ferrite nanoparticles
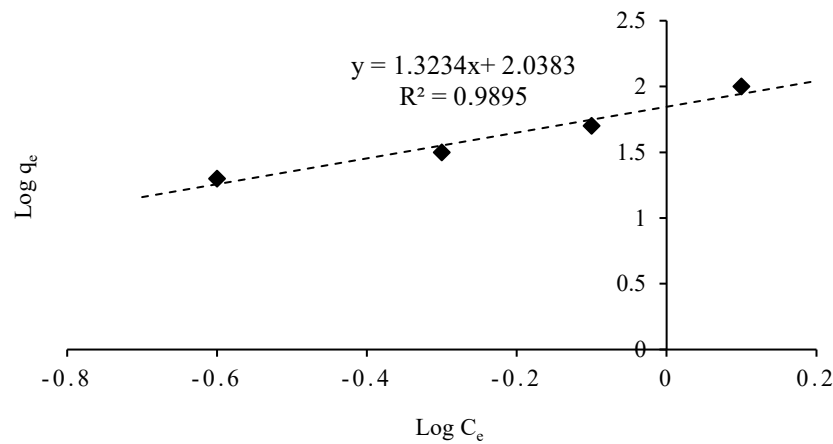

Fig. 12. Freundlich isotherm diagram of copper adsorption by manganese ferrite nanoparticles

Table 3. Langmuir and Freundlich equations for the adsorption isotherm of the Langmuir equation

Langmuir Equation	R^2	b(l/mg)	q_m(mg/g)
Y=-0.0059x+0.0151	0.9574	390.0	49.169
Freundlich equations	R^2	n	k_f
Y=1.3234x+2.0383	0.9895	755.0	219.109

these nanoparticles follow a pseudo-second-order model [28].

Adsorption Isotherms

Isotherms show the relationship between the concentration of adsorbent in solution and the amount of absorbed substance on the adsorbent at a constant temperature [19,20].

Figs. 11 and 12 indicate the Langmuir and Freundlich adsorption isotherms. The parameters related to these isotherms are presented in Table 3. In these figures, a high value of R or coefficient of determination indicates that the experimental data follow both the Langmuir and Freundlich equations. Nevertheless, the Freundlich model fits the test data better due to the higher value of R^2. The closer the value of R^2 is to 1, the more the adsorption mechanism follows the model. Moreover, the maximum absorption capacity of Langmuir was 169.49 mg/g [7].

Lower doses of the absorbents with higher adsorption capacities are required for a certain amount of adsorption, which is considered an advantage. In addition, Yoming Ren et al. used manganese dioxide nanoparticles to adsorb copper and lead, which followed the Langmuir adsorption isotherm [9].

CONCLUSION

The results indicated that manganese ferrite nanoparticles at an optimal pH=7 significantly removed copper from water in a short time of approximately 1 h. With increasing the concentration of nanoparticles, the removal efficiency increased; however, the adsorption capacity decreased. The results of investigating the adsorption isotherms indicated that the Freundlich model is a better fit for the experimental data compared to the Langmuir model. Moreover, Kinetic studies indicated that the copper adsorption process is consistent with the pseudo-second-order kinetic model. In general, the results of this study revealed that the use of manganese ferrite nanoparticles is a new and effective technology to purify the water system of heavy metals such as copper.

CONFLICT OF INTEREST

The authors declare that there is no conflict of interests regarding the publication of this manuscript.

REFERENCES

1. Khan SH. Advanced approaches for heavy metals removal from industrial wastewater. New Trends in Removal of Heavy Metals from Industrial Wastewater: Elsevier; 2021. p. 403-440.
2. Xu J, Yang L, Wang Z, Dong G, Huang J, Wang Y. Toxicity of copper on rice growth and accumulation of copper in rice grain in copper contaminated soil. Chemosphere. 2006;62(4):602-607.
3. Rao G, Lu C, Su F. Sorption of divalent metal ions from aqueous solution by carbon nanotubes: A review. Sep Purif Technol. 2007;58(1):224-231.
4. Zhuang HL, Zheng GP, Soh AK. Interactions between transition metals and defective carbon nanotubes. Computational Materials Science. 2008;43(4):823-828.
5. Removal of Dimethyl Phthalate from Aqueous Solution by Synthetic Modified Nano Zeolite Using Cu₂O Nanoparticles. International Journal of Engineering. 2016;29(9).
6. Chen J-h, Wang Y-j, Zhou D-m, Cui Y-x, Wang S-q, Chen Y-c. Adsorption and desorption of Cu(II), Zn(II), Pb(II), and Cd(II) on the soils amended with nanoscale hydroxyapatite. Environmental Progress & Sustainable Energy. 2009;29(2):233-241.
7. Zaman MI, Mustafa S, Khan S, Xing B. Effect of phosphate complexation on Cd²⁺ sorption by manganese dioxide (β-MnO₂). Journal of Colloid and Interface Science. 2009;330(1):9-19.
8. Su Q, Pan B, Wan S, Zhang W, Lv L. Use of hydrous manganese dioxide as a potential sorbent for selective removal of lead, cadmium, and zinc ions from water. Journal of Colloid and Interface Science. 2010;349(2):607-612.
9. Ren Y, Yan N, Feng J, Ma J, Wen Q, Li N, et al. Adsorption mechanism of copper and lead ions onto graphene nanosheet/δ-MnO₂. Materials Chemistry and Physics. 2012;136(2-3):538-544.
10. Luo C, Wei R, Guo D, Zhang S, Yan S. Adsorption behavior of

MnO$_2$ functionalized multi-walled carbon nanotubes for the removal of cadmium from aqueous solutions. Chem Eng J. 2013;225:406-415.

11. Huang S-H, Chen D-H. Rapid removal of heavy metal cations and anions from aqueous solutions by an amino-functionalized magnetic nano-adsorbent. J Hazard Mater. 2009;163(1):174-179.

12. Langmuir I. THE CONSTITUTION AND FUNDAMENTAL PROPERTIES OF SOLIDS AND LIQUIDS. PART I. SOLIDS. Journal of the American Chemical Society. 1916;38(11):2221-2295.

13. Esfahani AR, Firouzi AF, Sayyad G, Kiasat A. Lead Removal from Aqueous Solutions Using Polyacrylicacid-Stabilized Zero-Valent Iron Nanoparticles. Research Journal of Environmental and Earth Sciences. 2013;5(9):548-555.

14. Dong L, Zhu Z, Ma H, Qiu Y, Zhao J. Simultaneous adsorption of lead and cadmium on MnO$_2$-loaded resin. Journal of Environmental Sciences. 2010;22(2):225-229.

15. IV.-ON THE SO-CALLED GENITIVE ABSOLUTE AND ITS USE ESPECIALLY IN THE ATTIC ORATORS. On the So-Called Genitive Absolute and Its Use Especially in the Attic Orators: Gorgias Press; 2009. p. 310-343.

16. Ho YS, Wase DAJ, Forster CF. Kinetic Studies of Competitive Heavy Metal Adsorption by Sphagnum Moss Peat. Environ Technol. 1996;17(1):71-77.

17. Hakami O, Zhang Y, Banks CJ. Thiol-functionalised mesoporous silica-coated magnetite nanoparticles for high efficiency removal and recovery of Hg from water. Water Res. 2012;46(12):3913-3922.

18. Song J, Kong H, Jang J. Adsorption of heavy metal ions from aqueous solution by polyrhodanine-encapsulated magnetic nanoparticles. Journal of Colloid and Interface Science. 2011;359(2):505-511.

19. Geng X, Zebolsky DM. The Stoichiometric Displacement Model and Langmuir and Freundlich Adsorption. J Chem Educ. 2002;79(3):385.

20. Byström AM, Lund EW, Lund LK, Hakala M. The Crystal Structure of Ramsdellite, an Orthorhombic Modification of MnO$_2$. Acta Chem Scand. 1949;3:163-173.

21. Author index. Bone Miner. 1993;21(3):245-246.

22. Ananth MV, Pethkar S, Dakshinamurthi K. Distortion of MnO$_6$ octahedra and electrochemical activity of Nstutite-based MnO$_2$ polymorphs for alkaline electrolytes—an FTIR study. J Power Sources. 1998;75(2):278-282.

23. Malkoc E, Nuhoglu Y. Investigations of nickel(II) removal from aqueous solutions using tea factory waste. J Hazard Mater. 2005;127(1-3):120-128.

24. Ozcan A, Ozcan A, Tunali S, Akar T, Kiran I. Determination of the equilibrium, kinetic and thermodynamic parameters of adsorption of copper(II) ions onto seeds of. J Hazard Mater. 2005;124(1-3):200-208.

25. Mobasherpour I, Salahi E, Pazouki M. Removal of divalent cadmium cations by means of synthetic nano crystallite hydroxyapatite. Desalination. 2011;266(1-3):142-148.

26. Herrero D, Arias PL, Cambra JF, Antuñano N. Studies on impurity iron removal from zinc electrolyte using MnO$_2$–H$_2$O$_2$. Hydrometallurgy. 2011;105(3-4):370-373.

27. Zhao D, Yang X, Zhang H, Chen C, Wang X. Effect of environmental conditions on Pb(II) adsorption on β-MnO$_2$. Chem Eng J. 2010;164(1):49-55.

28. Özacar M, Şengil İA. Adsorption of metal complex dyes from aqueous solutions by pine sawdust. Bioresour Technol. 2005;96(7):791-795.

29. Rawajfih Z, Nsour N. Thermodynamic analysis of sorption isotherms of chromium(VI) anionic species on reed biomass. The Journal of Chemical Thermodynamics. 2008;40(5):846-851.

30. Xu M, Wang H, Lei D, Qu D, Zhai Y, Wang Y. Removal of Pb(II) from aqueous solution by hydrous manganese dioxide: Adsorption behavior and mechanism. Journal of Environmental Sciences. 2013;25(3):479-486.

31. Maliyekkal SM, Lisha KP, Pradeep T. A novel cellulose–manganese oxide hybrid material by in situ soft chemical synthesis and its application for the removal of Pb(II) from water. J Hazard Mater. 2010;181(1-3):986-995.

32. Katal R, Hasani E, Farnam M, Baei MS, Ghayyem MA. Charcoal Ash as an Adsorbent for Ni(II) Adsorption and Its Application for Wastewater Treatment. Journal of Chemical & Engineering Data. 2012;57(2):374-383.

33. Munagapati VS, Yarramuthi V, Nadavala SK, Alla SR, Abburi K. Biosorption of Cu(II), Cd(II) and Pb(II) by Acacia leucocephala bark powder: Kinetics, equilibrium and thermodynamics. Chem Eng J. 2010;157(2-3):357-365.

34. Keskinkan O, Goksu MZL, Basibuyuk M, Forster CF. Heavy metal adsorption properties of a submerged aquatic plant (Ceratophyllum demersum). Bioresour Technol. 2004;92(2):197-200.

35. Amini M, Ostadsharif M, Naghsh N. Effects of magnetic hydroethanolic extract of Nigella sativa and magnesium oxide nanoparticles (MgO) on catalase gene expression in liver of diabetic male rats. MEDICAL SCIENCES JOURNAL. 2022;32(2):123-131.